was allowed to warm to 0 °C, and stirring was continued for 30 min. A 0.64-mL aliquot of this solution was removed and added to 20.6 mg (0.064 mmol) of **11**-^{79}Br. The solution was cooled to −98 °C by the use of a 50:50 methanol:pentane/N_2 bath; 0.070 mL of *tert*-butyllithium (1.65 M in pentane, 0.115 mmol) was added. The solution was held at −98 °C for 20 min, and 0.1 mL (2.5 mmol) of methanol was added. The solution was stirred at −98 °C for an additional 20 min, after which the cooling bath was removed. After the solution was warmed to room temperature, water was added, and the THF/methanol was removed in vacuo. The aqueous mixture was extracted with Et_2O (three 5-mL portions), and the combined organic extract was washed with brine and dried with $MgSO_4$. The drying agent was removed by filtration, and the solvent was removed in vacuo to yield 13.5 mg of a pale yellow oil. The crude product mixture was analyzed by GC/EIMS for the isotopic composition of **15**. The GC/EIMS peak intensities for **15** as well as the peak intensities for the starting material **11**-^{79}Br are given in the supplemental material.

Reaction of 12-^{79}Br and 12-$^{81}BrD_2$ with *tert*-Butyllithium, 0.1 M. Endocyclic Restriction Test of 12. To a solution of 8.0 mg of **12**-^{79}Br and 7.6 mg of **12**-$^{81}BrD_2$ (0.0441 mmol total) in 0.44 mL of THF, cooled to −98 °C by the use of a 50:50 methanol:pentane/N_2 bath, was added 0.055 mL of *tert*-butyllithium (1.42 M in pentane, 0.079 mmol). The solution was held at −98 °C for 20 min, and 0.1 mL (2.5 mmol) of methanol was added. The solution was stirred at −98 °C for an additional 20 min, after which the cooling bath was removed. After the solution was warmed to room temperature, water was added, and the THF/methanol was removed in vacuo. The aqueous mixture was extracted with Et_2O (three 5-mL portions), and the combined organic extract was washed with brine and dried with $MgSO_4$. The drying agent was removed by filtration, and the solvent was removed in vacuo to yield 14.0 mg of a pale yellow oil. The crude product mixture was analyzed by capillary GC for its composition of **19–23** and **12** and by GC/EIMS for the isotopic composition of **19–21** and recovered **12**. The GC/EIMS peak intensities for **19–21** and recovered **12**, as well as the peak intensities for the starting material mixture, are given in the supplemental material.

Reaction of 12-^{79}Br in the Presence of LiBr. To a solution of 0.09 mL (1.0 mmol) of 1,2-dibromoethane in 10 mL of THF at −78 °C was added 1.68 mL of *n*-butyllithium (1.68 M in hexanes, 1.0 mmol). The solution was allowed to warm to 0 °C, and stirring was continued for 30 min. A 0.37-mL aliquot of this solution was removed, and added to 11.4 mg (0.037 mmol) of **12**-^{79}Br. The solution was cooled to −98 °C by the use of a 50:50 methanol:pentane/N_2 bath; 0.037 mL of *tert*-butyllithium (1.80 M in pentane, 0.067 mmol) was added. The solution was held at −98 °C for 20 min, and 0.1 mL (2.5 mmol) of methanol was added. The solution was stirred at −98 °C for an additional 20 min, after which the cooling bath was removed. After the solution was warmed to room temperature, water was added, and the THF/methanol was removed in vacuo. The aqueous mixture was extracted with Et_2O (three 5-mL portions), and the combined organic extract was washed with brine and dried with $MgSO_4$. The drying agent was removed by filtration, and the solvent was removed in vacuo to yield 8.2 mg of a pale yellow oil. The crude product mixture was analyzed by GC/EIMS for the isotopic composition of **20**. The GC/EIMS peak intensities for **20** as well as the peak intensities for the starting material **12**-^{79}Br are given in the supplemental material.

Reaction of 13-^{79}Br and 13-$^{81}BrD_2$ with *tert*-Butyllithium, 0.02 M. Endocyclic Restriction Test of 13. To a solution of 21.9 mg of **13**-^{79}Br and 21.4 mg of **13**-$^{81}BrD_2$ (0.107 mmol total) in 5.4 mL of THF, cooled to −98 °C by the use of a 50:50 methanol:pentane/N_2 bath, was added 0.12 mL of *tert*-butyllithium (1.55 M in pentane, 0.19 mmol). The solution was held at −98 °C for 30 min, and 0.1 mL (2.5 mmol) of methanol was added. The solution was stirred at −98 °C for an additional 20 min, after which the cooling bath was removed. After the solution was warmed to room temperature, water was added, and the THF/methanol was removed in vacuo. The aqueous mixture was extracted with Et_2O (three 5-mL portions), and the combined organic extract was washed with brine and dried with $MgSO_4$. The drying agent was removed by filtration, and the solvent was removed in vacuo to yield 35.2 mg of a pale yellow oil. The crude product mixture was analyzed by capillary GC for its composition of **24–30** and **13** and by GC/FIMS for the isotopic composition of **24**, **26**, **27**, and recovered **13**. The GC/FIMS peak intensities for **24**, **26**, **27**, and recovered **13** as well as the peak intensities for the starting material mixture are given in the supplemental material.

Reaction of 13-^{79}Br and 13-$^{81}BrD_2$ with *tert*-Butyllithium, 0.001 M. Endocyclic Restriction Test of 13. To a solution of 8.1 mg of **13**-^{79}Br and 8.1 mg of **13**-$^{81}BrD_2$ (0.0327 mmol total) in 32.7 mL of THF, cooled to −98 °C by the use of a 50:50 methanol:pentane/N_2 bath, was added 0.038 mL of *tert*-butyllithium (1.55 M in pentane, 0.059 mmol). The solution was held at −98 °C for 40 min, and 0.5 mL (12.5 mmol) of methanol was added. The solution was stirred at −98 °C for an additional 20 min, after which the cooling bath was removed. After the solution was warmed to room temperature, water was added, and the THF/methanol was removed in vacuo. The aqueous mixture was extracted with Et_2O (three 5-mL portions), and the combined organic extract was washed with brine and dried with $MgSO_4$. The drying agent was removed by filtration, and the solvent was removed in vacuo to yield 5.1 mg of a pale yellow oil. The crude product mixture was analyzed by capillary GC for its composition of **24–30** and **13**, and by GC/FIMS for the isotopic composition of **24**, **26**, **27**, and recovered **13**. The GC/FIMS peak intensities for **24**, **26**, **27**, and recovered **13**, as well as the peak intensities for the starting material mixture are given in the supplemental material.

Acknowledgment. We are grateful to Dr. Richard Milberg and the Mass Spectrometry Facility at UIUC for analyses of isotopic composition. We are grateful to the National Science Foundation and the National Institutes of Health for support of this work.

Supplementary Material Available: The data for the mass spectral analyses and the syntheses of isotopically substituted **11**, **12**, and **13** (36 pages). Ordering information is given on any current masthead page.

Reaction of (*E*)-*O*-Arylbenzaldoximes with Sodium Methoxide in Methanol. Effect of Leaving Group upon Nitrile-Forming Transition State

Bong Rae Cho,* Jinhee Jung, and Eun Kyung Ahn

Contribution from the Department of Chemistry, Korea University, 1-Anamdong, Seoul 136-701, Korea. *Received October 1, 1991*

Abstract: Reactions of (*E*)-*O*-arylbenzaldoximes **1–3** with MeONa–MeOH have been studied kinetically. The reactions proceed via competing E2 and S_NAr reactions, in which the first step is rate-determining. Although the reactions were strongly influenced by the electronic effect of the β- and *O*-aryl substituents, they were insensitive to the steric effect of the *O*-aryl group, except that the S_NAr reaction was retarded by the CF_3 group of **2**. For eliminations from **1–3** promoted by MeONa–MeOH, the k_H/k_D value increased and the Hammett ρ value decreased with better leaving groups. From these results, the effect of leaving group variation upon the nitrile-forming transition state is assessed.

Recently we reported a kinetic investigation of the nitrile-forming elimination from (*E*)-*O*-arylbenzaldoximes promoted by tertiary amines in MeCN.[1] The reactions proceeded via an E2 central type of transition state with similar extents of C_β–H and

0002-7863/92/1514-3425$03.00/0

Table I. Lengths of C_β–H, C=N, N_α–O, and O–Ar Bonds in (*E*)-PhCH=NOC$_6$H$_2$(NO$_2$)$_2$R Determined by X-ray Diffraction

	bond length, Å			
R	C_β–H	C=N	N_α–O	O–Ar
H[a]	1.139	1.266	1.431	1.354
CF_3	1.10	1.269	1.440	1.356
NO_2	0.96	1.261	1.436	1.343

[a] Average of two alternating structures.

N_α–OAr bond cleavage, extensive triple-bond formation, and equal negative charge distribution between the β-carbon and the leaving group. The transition state was shifted toward the E1cb corner by an electron-withdrawing β-aryl substituent and toward the E1 intermediate and the product by a stronger base in the reaction coordinate diagram. On the other hand, when the leaving group was changed from 2,4-dinitrophenoxide to picrate, the ρ value decreased but the β value increased. The results are in conflict with the prediction of the reaction coordinate diagram that both ρ and β values should decrease with a better leaving group.[2a]

The unusual changes in the transition state structure could result from either the large difference in leaving group abilities or the steric effect. If the reactivity difference is too large, there may be profound change in the potential energy surface preventing one from starting at **1** and predicting the structural effects in **3** on the transition state. However, the validity of this interpretation remains to be verified. Alternatively, if the N–OAr bond is lengthened by the steric effect between the imino nitrogen and the ortho nitro substituents of the picrate leaving group, the compound could become more reactive than expected from its electonic effect, which may also cause such unusual change. In order to determine which of these factors might be responsible for the unusual change in the transition state, we have investigated the reactions of (*E*)-*O*-arylbenzaldoximes **1–3** with MeONa in MeOH (eq 1). It was expected that the difference in leaving

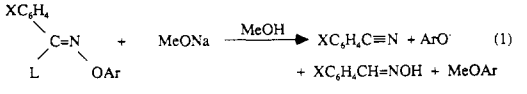

(1)

Ar

1 2,4-dinitrophenyl
2 2,4-dinitro-6-trifluoromethylphenyl
3 picryl

a L = H, X = H
b L = D, X = H
c L = H, X = *p*-CH$_3$O
d L = H, X = *m*-Br
e L = H, X = *p*-NO$_2$

group abilities could be decreased by utilizing 2,4-dinitro-6-(trifluoromethyl)phenoxide, whose pK_a value is in between those for 2,4-dinitrophenoxide and picrate,[3] as an additional leaving group. The difference could be further decreased by employing MeONa–MeOH as the base–solvent system because the ΔpK_a values for the aryl oxides are smaller in protic than in aprotic solvents.[6] Thus, if the large difference in leaving group ability were the origin of the unusual leaving group effect, a normal effect should be observed for these reactions. Furthermore, the steric effect of the leaving group could also be assessed by comparing the structures and the kinetic data for **1–3**.

In this work, we have determined the mechanism and the influence of the substrate structure upon the reactions of **1–3** with MeONa in MeOH. The effect of leaving group variation on the nitrile-forming transition state has been investigated to assess the origin of the unusual leaving group effect observed for R_3N-promoted eliminations from **1** and **3**. The results of these studies are reported here.

Table II. Yields and Rate Constants for Reaction of (*E*)-ArCH=NOC$_6$H$_3$-2,4-(NO$_2$)$_2$ with MeONa–MeOH

compd[a]	temp, °C	10^2[MeONa], M	E2 yield,[b] %	$10^2k_2^{E}$,[c,d] M^{-1} s^{-1}	10^2k_A,[d,e] M^{-1} s^{-1}
1a	25.0	9.67	77.2	8.77	2.47
1a	25.0	0.967	77.6	7.60	2.14
1a	35.0	9.67	79.1	22.5	6.34
1a	45.0	9.67	80.7	58.0	16.4
1b	25.0	9.67	52.4	2.71	
1c	25.0	9.67	58.7	2.52	1.85
1d	25.0	9.67	84.6	45.5	5.06
1e	25.0	3.22	100	324	

[a] [Substrate] = (5.0×10^{-5})–(1.0×10^{-4}) M. [b] Estimated uncertainty, ±3%. [c] $k_2^E = k_{obsd} \times$ E2 yield/[MeONa]. [d] Estimated uncertainty, ±5%. [e] $k_A = k_{obsd} \times S_NAr$ yield/[MeONa].

Table III. Yields and Rate Constants for Reaction of (*E*)-ArCH=NOC$_6$H$_2$-2,4-(NO$_2$)$_2$-6-CF$_3$ with MeONa–MeOH

compd[a]	temp, °C	10^3[MeONa], M	E2 yield,[b] %	k_2^{E},[c,d] M^{-1} s^{-1}	k_A,[d,e] M^{-1} s^{-1}
2a	25.0	7.25	90.1	2.63	0.465
2a	25.0	0.967	87.3	2.53	0.446
2a	35.0	7.25	86.4	5.83	1.03
2a	45.0	7.25	86.7	12.7	2.23
2b	25.0	7.25	56.5	0.738	
2c	25.0	7.25	78.7	0.907	0.302
2d	25.0	7.25	94.2	11.1	1.24
2e	25.0	7.25	100	60.9	

[a] [Substrate] = (5.0×10^{-5})–(1.0×10^{-4}) M. [b] Estimated uncertainty, ±3%. [c] $k_2^E = k_{obsd} \times$ E2 yield/[MeONa]. [d] Estimated uncertainty, ±5%. [e] $k_A = k_{obsd} \times S_NAr$ yield/[MeONa].

Table IV. Yields and Rate Constants for Reaction of (*E*)-ArCH=NOPic with MeONa–MeOH

compd[a]	temp, °C	10^4[MeONa], M	E2 yield,[b] %	k_2^{E},[c,d] M^{-1} s^{-1}	k_A,[d,e] M^{-1} s^{-1}
3a	25.0	96.7	32.0	10.6	23.6
3a	25.0	9.67	30.1	10.6	23.5
3a	35.0	9.67	34.4	22.0	42.8
3a	45.0	9.67	35.3	47.7	81.2
3b	25.0	9.67	13.6	2.67	
3c	25.0	9.67	26.5	5.19	15.6
3d	25.0	9.67	53.2	35.5	30.2
3e	25.0	9.67	82.7	188	

[a] [Substrate] = (5.0×10^{-5})–(1.0×10^{-4}) M. [b] Estimated uncertainty, ±3%. [c] $k_2^E = k_{obsd} \times$ E2 yield/[MeONa]. [d] Estimated uncertainty, ±5%. [e] $k_A = k_{obsd} \times S_NAr$ yield/[MeONa].

Results

(*E*)-*O*-Arylbenzaldoximes **1–3** were prepared by the reactions of (*E*)-benzaldoximes with aryl halides as reported previously.[1] The spectral and analytical data for the new compounds were consistent with the proposed structures. The X-ray structures of **1a–3a** are nearly planar except that the ortho nitro groups adjacent to the imino nitrogen in **2a** and **3a** are perpendicular to the *O*-aryl ring. The lengths of the C_β–H, C=N, N—O, and O—Ar bonds are listed in Table I.

Reactions of **1–3** with MeONa in MeOH produced benzonitrile, aryl oxides, benzaldoximes, and anisoles. 2,4-Dinitro-6-(trifluoromethyl)anisole and methyl picrate reacted further with MeONa to produce the Meisenheimer complexes under the reaction conditions.

The rates of reactions were followed by measuring the disappearance of absorption of the substrates in the region 292–314 nm. Pseudo-first-order conditions were employed. Excellent

(1) Cho, B. R.; Kim, K. D.; Lee, J. C.; Cho, N. S. *J. Am. Chem. Soc.* **1988**, *110*, 6145–6148.
(2) Lowry, T. H.; Richardson, K. S. *Mechanism and Theory in Organic Chemistry*; Harper and Row: New York, 1987; (a) pp 214–218, (b) pp 591–560, (c) pp 640–644.
(3) Estimated to be 1.70 from the linear relationship between the pK_a values of phenols and σ constants of the substituents.[4,5]
(4) Charton, M. *Prog. Phys. Org. Chem.* **1971**, *8*, 235–318.
(5) Hine, J. *Structural Effect on Equilibria in Organic Chemistry*; Wiley: New York, 1975; pp 80, 90.
(6) Coetzee, J. F. *Prog. Phys. Org. Chem.* **1965**, *4*, 45–92.
(7) Gandler, J. R.; Jencks, W. P. *J. Am. Chem. Soc.* **1982**, *104*, 1937–1951.
(8) Rochester, C. H.; Rossal, B. *Trans. Faraday Soc.* **1969**, *65*, 1004–1013.

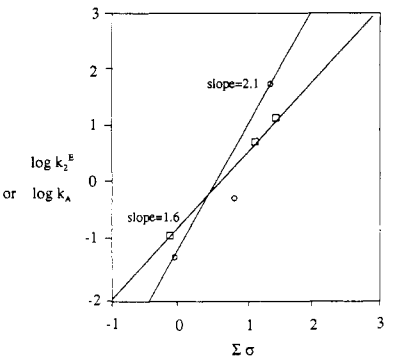

Figure 1. Hammett plots for E2 (□) and S_NAr (○) reactions of (*E*)-*O*-arylbenzaldoximes with MeONa in MeOH.

Table V. Transition State Parameters for Nitrile-Forming Elimination from (*E*)-ArCH=NOC$_6$H$_3$-2,4-(NO$_2$)$_2$ under Various Conditions

base–solvent	•OH–60% DMSO(aq)[a]	MeO⁻–MeOH	Et$_3$N–MeCN[b]
pK_a	18.3[c]	18.3[d]	18.5[e]
rel rate	1	0.02	0.0001
ρ	0.2 ± 0.5	2.0 ± 0.0	2.6 ± 0.2
β	0.49 ± 0.14	0.5[f]	0.57 ± 0.12
ρ_{lg}	1.4 ± 0.1	1.6 ± 0.0	2.6
β_{lg}	−0.59 ± 0.01	−0.62 ± 0.00	0.65
$\Delta H^{\ddagger}$	14.5 ± 0.1	17.5 ± 0.2	13.9 ± 0.8
$\Delta S^{\ddagger}$	−6.4 ± 0.1	−4.8 ± 0.7	−28.1 ± 2.2
$\Delta G^{\ddagger}$	16.4 ± 0.1	18.9 ± 0.2	22.3 ± 1.8

[a] Reference 12. [b] Reference 1. [c] Reference 7. [d] Reference 8. [e] Reference 6. [f] Estimated from k_H/k_D value.

Table VI. Effect of Leaving Group upon Nitrile-Forming Elimination from (*E*)-ArCH=NOC$_6$H$_2$-2,4-(NO$_2$)$_2$-6-R Promoted by MeONa–MeOH

	R = H	R = CF$_3$	R = NO$_2$
pK_{lg}	4.11[a]	1.70[b]	0.71[a]
rel rate	1	31	125
ρ	2.0 ± 0.1	1.7 ± 0.1	1.5 ± 0.1
k_H/k_D	3.1	3.6	4.0
$\Delta H^{\ddagger}$	17.5 ± 0.2	14.1 ± 0.1	13.8 ± 0.3
$\Delta S^{\ddagger}$	−4.6 ± 0.7	−9.1 ± 0.3	−7.6 ± 0.9
$\Delta G^{\ddagger}$	18.9 ± 0.2	16.8 ± 0.1	16.0 ± 0.3

[a] Reference 6. [b] Reference 3.

pseudo-first-order kinetic plots which covered at least 2 half-lives were obtained. For reactions of **1** and **2** with MeONa in MeOH, the increase in absorption at 356 nm was also measured. The rate constants determined by these two methods were always identical. However, for reactions of **2** at [MeONa] > 0.03 M and of **3** at all base concentrations, the increase in the absorption of the aryl oxides could not be monitored because the kinetics were complicated by the formation of the Meisenheimer complexes. The observed rate constants were multiplied by the product yields (vide infra) to determine the rate coefficients for the elimination and the S_NAr processes. The k_2^E and k_A values were calculated by dividing the corresponding rate constants by base concentration. The rate constants are summarized in Tables II–IV.

Comparison of the absorption in infinity samples with that for authentic samples of the products allowed the product yield to be calculated. The yields remained constant with base concentration variation but were strongly influenced by the β- and *O*-aryl substituents. The product yields are summarized in Tables II–IV.

The influence of β-aryl substituents upon the elimination and substitution rates correlated satisfactorily with the Hammett equation using σ values (plots not shown). For reactions of **1–3**, Hammett ρ values for the elimination and S_NAr processes are 2.0, 1.7, and 1.5 and 0.68, 0.94, and 0.43, respectively. Similarly, the elimination rates determined with different *O*-aryl substituents were correlated with $\sum\sigma = \sigma_0 + \sigma_P^-$ values (Figure 1), where σ_0 constants were calculated by the literature method.[4] On the other hand, the k_A value for the S_NAr reaction of **2a** showed a large negative deviation from the Hammett plot. Therefore, the Hammett ρ_{lg} values for the S_NAr reaction with the *O*-aryl group variation were calculated without the data for **2a**. The ρ_{lg} values are 1.6 and 2.1 for the elimination and S_NAr pathways, respectively.

Scheme I

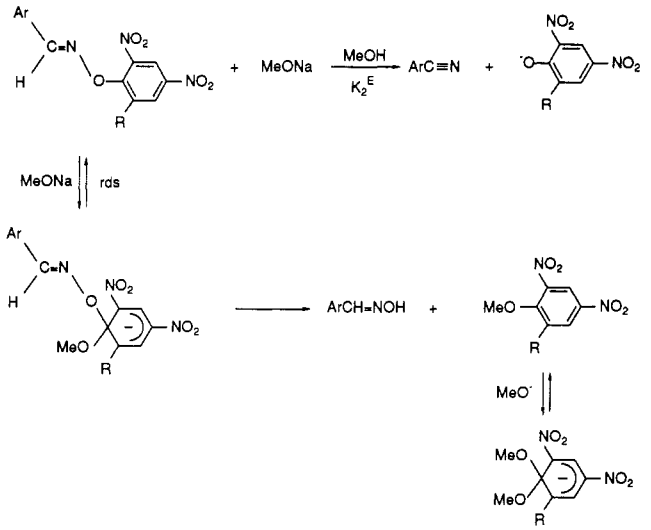

Rates of elimination from **1–3** promoted by MeONa–MeOH were measured at three temperatures spanning 20 °C. Arrhenius plots exhibited excellent linearity. Calculated enthalpies and entropies of activation are listed in Tables V and VI.

From the rate coefficients for elimination from **1a–3a** and their deuterated analogues **1b–3b**, primary deuterium isotope effect values were calculated. The values are 3.1, 3.6, and 4.0 for **1a**, **2a**, and **3a**, respectively (Table VI).

Discussion

Mechanism and the Effect of Substrate Structure upon the Reactions of 1–3. Earlier it was established that the reactions of **1** and **3** with R_3N in MeCN proceeded by an E2 mechanism.[1] On the other hand, when the same substrates were allowed to react with R_2NH in MeCN, the reactions proceeded by competing E2 and S_NAr mechanisms in which the second step was rate-determining.[9] The results of kinetic and product studies reveal that the reactions of **1–3** with MeONa in MeOH also proceed by a similar mechanism. Since the elimination reactions exhibit second-order kinetics and substantial values for primary isotope effect and β_{lg} are determined, all but the E2 mechanism can be ruled out.[2b,10] In addition, the observation of simple second-order kinetics for the S_NAr reaction is consistent with an addition–elimination mechanism, in which the first step is rate-determining (Scheme I).[2c,11]

Comparison of the yield data and Hammett ρ values reveals that the E2 reaction is more sensitive than the S_NAr reactions to the variation of the β-aryl substituent. The yield of elimination product increases with the electron-withdrawing ability of the β-aryl substituent (Tables II–IV). Moreover, the Hammett ρ values for the elimination reactions are much greater than those for the S_NAr reactions (vide supra). The results can be readily explained by the relative distance between the substituent and the reaction sites. Since the C_β–H bond is parallel to the β-aryl ring and the first step of the S_NAr mechanism is assumed to be rate-determining, the β-aryl substituent is expected to influence the rates of both E2 and S_NAr reactions primarily through inductive effect. Therefore, the E2 reaction must be more sensitive

(9) Cho, B. R.; Min, B. K.; Lee, C. W.; Je, J. T. *J. Org. Chem.* **1991**, *56*, 5513–5517.
(10) Gandler, J. R. In *The Chemistry of Double Bonded Functional Groups*; Patai, S., Ed.; Wiley: Chichester, 1989; Vol. 2, Part 1, pp 734–797.
(11) Terrier, F. *Chem. Rev.* **1982**, *82*, 78–152.

to the electron-withdrawing ability of the β-aryl substituent than the S_NAr reaction because the substituent is closer to the C_β–H bond than to the *O*-aryl ring.

In contrast, the S_NAr reaction appears to be more sensitive to the variation of the *O*-aryl substituent as indicated by the decrease in E2 yield with the change of substrate from **1** to **3** (Tables II–IV) and the greater ρ_{lg} value for the S_NAr reaction (Figure 1). An electron-withdrawing substituent at the *O*-aryl ring is expected to increase the rates of both E2 and S_NAr reactions by stabilizing the negative charge that develops in the *O*-aryl ring and at the oxygen atom of the aryl oxide in the respective transition states. However, this effect would be greater for the S_NAr reaction because the substituent is closer to the former than to the latter.

The large negative deviation of the S_NAr rate for **2a** from the Hammett plot (Figure 1) and the higher yield of E2 reaction product for **2** (Table III) can be attributed to the steric effect. Although the geometries of the ortho nitro groups in **1a–3a** differ with respect to the *O*-aryl ring (vide supra), they are not expected to influence the S_NAr reactions sterically because they can rotate in the intermediate to relieve the steric strain as they do in the reactant. However, the steric effect of the spherical CF_3 group cannot be alleviated in a similar manner. Therefore, the rate of the S_NAr reaction for **2a** could be slower and the yield of the E2 product lower than expected from its electronic effect.

Transition State Structure for Elimination from 1. The transition state parameters for eliminations from **1** promoted by $^-$OH–60% DMSO (aqueous),[12] MeONa–MeOH, and Et_3N–MeCN[1] are compared in Table V. The result reveals that there is a small but clear trend in the structures of the transition states with this variation of the base–solvent system. Hammett ρ and ρ_{lg} values increase with the same base–solvent variation, indicating a gradual increase in the negative charge development on the β-carbon and the leaving group. An increase in the cleavage of the C_β–H and N_α–OAr bonds is also indicated by the increase in the β and $|\beta_{lg}|$ values in the same order. Thus it appears that the structure of the transition states for MeONa-promoted eliminations from **1** is in between those for $^-$OH- and Et_3N-promoted eliminations from the same substrate. Since it has been established that the latter two reactions proceed via an E2 central transition state,[1,12] the transition state structure of the former reaction can also be assumed to be E2 central with significant cleavage of the C_β–H and N_α–OAr bonds, extensive triple-bond formation, and similar negative charge development on the β-carbon and the leaving group oxygen atom.

The change in the transition state structure with variation in the base–solvent system can be attributed to the change in reactivity and the solvent effect. Since the base–solvent system becomes progressively less reactive, the transition state should become more productlike with a greater extent of C_β–H and N_αOAr bond rupture and more negative charge development. Moreover, the increase in the carbanionic character would be amplified in MeCN, because the partial negative charge developed in the transition state cannot be stabilized in this poorly anion-solvating medium. Thus, although the 50-fold decrease in rate with the change from $^-$OH–60% DMSO (aqueous) to MeONa–MeOH can be attributed to the higher enthalpy of activation, the large rate retardation with Et_3N–MeCN as the base–solvent system must result from an entropic factor.

Effect of Leaving Group upon Nitrile-Forming Transition State. The main objective of present study is to determine whether the leaving group steric effects or the large difference in leaving group abilities might be the origin of the unusual leaving group effect observed for Et_3N-promoted eliminations from **1** and **3**.

The possibility of the leaving group steric effect for the origin of the unusual effect has been ruled out by the X-ray structure and Hammett plot (Figure 1). The structures of **1a–3a** are very similar except that the ortho nitro groups adjacent to the imino nitrogen in **2a** and **3a** are perpendicular to the *O*-aryl ring and the C_β–H bond in **3a** is approximately 0.1 Å shorter than the corresponding bonds in **1a** and **2a** (Table I). Since the base would attack the C_β–H bond, which is away from the *O*-aryl group, and both the C_β–H and N_α–OAr bonds would be lengthened in the transition state, the elimination reactions are not likely to be influenced significantly by this minor variation of the steric effect.

The absence of steric effect is clearly demonstrated by the excellent linearity of the Hammett plot for the elimination reactions with the leaving group variation (Figure 1). If the reactions were significantly influenced by the steric effect, a positive deviation should have been observed for sterically less congested **1a** in the Hammett plot. Furthermore, the excellent correlation of the elimination rates with the $\sum\sigma$ values, which take into account both inductive and resonance effects of the substituents,[4] indicates that the ortho nitro groups, which are perpendicular to the *O*-aryl group in **2** and **3**, must be coplanar with the aryl ring in the transition state. It appears that the steric effect of the ortho substituents in the reactants is completely lost in the transition state, presumably because the N–OAr bonds are sufficiently stretched enough in the transition state to relieve the steric strain between the ortho nitro group and the imino nitrogen. Assuming similar transition state structures for MeONa- and Et_3N-promoted eliminations from **1** (vide supra), it appears highly unlikely that the leaving group steric effect would cause such an unusual change in the transition state structure for the latter.

The transition state parameters for eliminations from **1–3** are summarized in Table VI. Hammett ρ values decrease as the leaving group becomes better, indicating a decrease in the carbanionic character on the β-carbon in the transition state. On the other hand, the k_H/k_D value increases in the same order. The increase in the k_H/k_D value with better leaving groups can be interpreted with either an increase or a decrease in the C–H bond rupture in the transition state.[13] However, since the maximum k_H/k_D is expected for 0.4 proton transfer[14] and the k_H/k_D value of 1.4–4.6 observed for alkoxide-promoted eliminations from vinyl halides has been interpreted with a proton transfer that is past the midpoint,[15] the k_H/k_D value of 3.1 for **1** should indicate more than 0.4 proton transfer in the transition state. Therefore, the latter interpretation appears more consistent with the experimental data. The decrease in carbanionic character on the β-carbon and the C_β–H bond cleavage with better leaving group ability are in perfect agreement with the prediction by the reaction coordinate diagram.[2a] It is clearly demonstrated that the effect of leaving group upon the nitrile-forming transition state becomes normal when the reactivity difference is modest. Therefore, it may be concluded that the unusual change in the transition state for R_3N-promoted eliminations from **1** and **3** in MeCN results from the large difference in the leaving group abilities. This result indicates a limitation of the More–O'Ferall–Jencks reaction coordinate diagram in that it cannot explain the structure–reactivity relationship of the elimination reactions when the reactivity difference is too large, although it is very successful for reactions with modest differences in reactivity.[16–18]

Experimental Section

Materials. (*E*)-*O*-Arylbenzaldoximes **1–3** were prepared by reactions of (*E*)-benzaldoximes with the appropriate aryl halides.[1] The physical, spectral, and analytical data for these compounds were consistent with the proposed structures. The melting point (°C), NMR (acetone-d_6, benzal C–H, ppm), IR (KBr, C=N, cm^{-1}), and analytical data of the new compounds are as follows. $C_6H_5CH{=}NOC_6H_2$-2,4-$(NO_2)_2$-6-CF_3 (**2a**) 153–154/8.8/1610. Anal. Calcd for $C_{14}H_8F_3N_3O_5$: C, 47.36; H, 2.43; N, 11.84. Found: C, 46.94; H, 2.13; N, 11.76. *p*-$CH_3OC_6H_4CH{=}NOC_6H_2$-2,4-$(NO_2)_2$-6-CF_3 (**2c**) 128/8.4/1620. Anal. Calcd for $C_{15}H_{10}F_3N_3O_6$: C, 46.69; H, 2.61; N, 10.90. Found: C, 46.59;

(12) Cho, B. R.; Lee, J. C.; Cho, N. S.; Kim, K. D. *J. Chem. Soc., Perkin Trans. 2* **1989**, 489–452.

(13) Smith, P. J. *In Isotopes in Organic Chemistry*, Buncel, E., Lee, C. C., Eds.; Elsevier: Amsterdam, 1976, pp 239–241.

(14) Saunders, W. H., Jr. *Chem. Scr.* **1975**, *8*, 27–36.

(15) Saunders, W. H., Jr.; Cockerill, A. F. *Mechanism of Elimination Reactions*; Wiley: New York, 1973; pp 510–518.

(16) Jencks, W. P. *Chem. Rev.* **1985**, *85*, 511–527.

(17) Baciocchi, E. *Acc. Chem. Res.* **1979**, *12*, 430–436.

(18) Hoffman, R. V.; Bartsch, R. A.; Cho, B. R. *Acc. Chem. Res.* **1989**, *22*, 211–217.

H, 2.50; H, 10.66. *m*-$BrC_6H_4CH{=}NOC_6H_2$-2,4-$(NO_2)_2$-6-CF_3 (**2d**) 132/8.8/1640. Anal. Calcd for $C_{14}H_7BrF_3N_3O_5$: C, 38.73; H, 1.63; N, 9.68. Found: C, 39.08; H, 1.64; N, 9.76. *p*-$NO_2C_6H_3CH{=}NOC_6H_2$-2,4-$(NO_2)_2$-6-CF_3 (**2e**) 138-141/9.0/1620. Anal. Calcd for $C_{14}H_7F_3N_4O_7$: C, 42.01; H, 1.76; N, 14.00. Found: C, 41.62; H, 1.58; N, 14.00.

The PhCD=NOAr compounds **1b-3b** were prepared by the reactions of PhCD=NOH with aryl halides. The proton magnetic resonance spectra (acetone-d_6) of PhCD=NOAr were exactly the same as those for PhCH=NOAr (**1a-3a**) except for the complete absence of the benzal C-H singlet of the latter at 8.5-8.8 ppm.

2,4-Dinitroanisole, 2,4-dinitro-6-(trifluoromethyl)anisole, and methyl picrate were prepared by reaction of the appropriate aryl oxide with MeONa-MeOH.

Methanol was purified as described previously. Solutions of MeO-Na-MeOH were prepared by adding clean pieces of sodium metal to anhydrous MeOH under nitrogen.

X-ray Structure Determination. The X-ray structure determinations of **1a-3a** were performed by Lucky Central Research Institute, Dae Jeon, Korea.

Ultraviolet Spectra of Reaction Products. λ_{max} and molar extinction coefficients of aryl oxides, anisoles, oximes, and Meisenheimer complexes in absolute MeOH were the following: 2,4-dinitrophenoxide, 356 nm (ϵ = 15 400); 2,4-dinitro-6-(trifluoromethyl)phenoxide, 348 nm (ϵ = 16 700); picrate, 354 nm (ϵ = 15 450); 2,4-dinitroanisole, 292 nm (ϵ = 11 200); 2,4-dinitro-6-(trifluoromethyl)anisole, 210 nm (ϵ = 16 400); methyl picrate, 220 nm (ϵ = 17 750); benzaldoxime, 292 nm (ϵ = 13 800); $[(CH_3O)_2C_6H_2$-2,4-$(NO_2)_2$-6-$CF_3]^-$, 472 nm (ϵ = 21 800); $[(CH_3O)_2C_6H_2$-2,4,6-$(NO_2)_3]^-$, 410 nm (ϵ = 24 700); $[(CH_3O)_2C_6H_2$-2,4-$(NO_2)_2$-6-$CF_3]^-$, 472 nm (ϵ = 21 800); $[(CH_3O)_2C_6H_2$-2,4,6-$(NO_2)_3]^-$, 410 nm (ϵ = 24 720).

Kinetic Studies. Reactions of **1-3** with MeONa-MeOH were followed using a Hewlett-Packard 8452 diode array spectrophotometer with thermostated cuvette holders under pseudo-first-order conditions employing at least a 10-fold excess of base. Reactions were initiated by injecting 5-10 μL of an ca. 10^{-2} M solution of substrate in acetonitrile into a cuvette containing 3.0 mL of MeONa-MeOH. Cuvettes were temperature equilibrated for at least 20 min prior to a kinetic run. All reactions were followed to completion. The decreases of the absorptions at 292, 298, and 314 nm for **1**, **2**, and **3**, respectively, with time were monitored. Plots of ln $(A_t - A_\infty)$ against time were linear over at least 2 half-lives or more of the reaction. The slope was the observed rate constant. For reactions of **1** and **2** with MeONa in MeOH, the increase in the absorption at 356 nm was also measured. The rates determined by these two methods were always identical. However, for reactions of **2** at [MeONa] > 0.03 M and of **3** at all base concentrations, the increases in the absorptions of the aryl oxides could not be monitored because the kinetics was complicated by the formation of the Meisenheimer complexes. The observed rate constants were multiplied by the product yields (vide infra) to determine the rate coefficients for the elimination and the S_NAr processes. The k_2^E and k_A values were calculated by dividing the corresponding rate constants by base concentration.

Product Studies. The products of the reactions of **1-3** with MeO-Na-MeOH were identified as described before.[1,9,12] The yields of the reaction products were determined by comparing the absorbance of the infinity samples from the kinetic reactions with those of authentic samples of the products.

Control Experiments. The stabilities of **1-3** were determined as reported earlier.[1]

Acknowledgment. This research was supported by Non Directed Research Fund, Korea Research Foundation, 1989, KOSEF, and OCRC-KOSEF.

Registry No. 1a, 75735-29-4; **1b**, 139584-37-5; **1c**, 115828-58-5; **1d**, 115828-59-6; **1e**, 75735-26-1; **2a**, 139584-38-6; **2b**, 139584-39-7; **2c**, 139584-40-0; **2d**, 139584-41-1; **2e**, 139584-42-2; **3a**, 115828-60-9; **3b**, 139584-43-3; **3c**, 115828-61-0; **3d**, 115828-62-1; **3e**, 115828-63-2; sodium methoxide, 124-41-4; benzaldehyde oxime, 622-31-1; benzaldehyde-α-*d* oxime, 14702-03-5; *p*-methoxybenzaldehyde oxime, 3717-21-3; *m*-bromobenzaldehyde oxime, 52739-46-5; *p*-nitrobenzaldehyde oxime, 3717-19-9; 2,4-dinitrophenyl chloride, 97-00-7; 2,4-dinitro-6-(trifluoromethyl)phenyl chloride, 392-95-0; picryl chloride, 88-88-0.

Materials Chemistry of Chiral Macromolecules. 1. Synthesis and Phase Transitions

J. S. Moore and S. I. Stupp*

Contribution from the Department of Materials Science and Engineering and Materials Research Laboratory, University of Illinois at Urbana-Champaign, Urbana, Illinois 61801.
Received November 23, 1990

Abstract: This paper describes work on synthesis of chiral macromolecules as part of a materials chemistry study which seeks to establish links in these systems among molecular structure, three-dimensional molecular organization, and properties. The basic materials chemistry hypothesis driving this work is that chiral forces among stereogenic centers may serve as guiding fields to organize polymers in two or three dimensions. It follows that physical properties could be directly or indirectly controlled by chirality. In order to promote strong forces among chiral centers the chains were designed to have stereogenic carbons substituted by the strongly dipolar cyano group and spaced by 16 atoms along the backbone. The preparative chemistry of chiral macromolecules is challenging given the limited number of polymerization methodologies and the inherent translational periodicity of synthetic polymers. We have synthesized here low symmetry chiral macromolecules in which the only symmetry element retained is polar translation; achiral homologues lacking the nitrile function, the configurationally disordered polymer, and dimeric model compounds were prepared as well. The compounds exhibited crystalline and liquid crystalline phases, and significant differences were observed among homologues through differential scanning calorimetry and optical microscopy. The substitution of nitrile groups every 16 atoms along the polymer backbone, specially with configurational disorder, leads to glassy or less ordered condensed phases. In some polymers when the strongly dipolar stereogenic centers do not have preferred handedness, chains organize into mesophases rather than crystalline structures. This is surprising since the concentration of stereogenic centers is extremely dilute. Using dimeric model compounds, homochiral recognition among stereogenic centers with large dipole moments was identified as an important factor in the assembly of molecules into layered structures. Interestingly, catenation of the dipolar stereogenic centers in polymeric compounds apparently leads to layered structures even when configurational disorder exists along the polymer backbone. This type of structural control could be extremely useful as an approach to tune physical properties of polymeric materials.

Introduction

The combination of chirality and polymeric dimension is ubiquitous in the molecules of nature, yet relatively few synthetic systems have been prepared and studied as three-dimensional molecular assemblies. Such systems have great potential as substrates for the discovery of new phenomena as well as new technically useful solid substances. Because of the many structures that could be achieved through isomeric forms of chiral polymers

0002-7863/92/1514-3429$03.00/0